Silva, Douglas Felipe da; Muraoka, Issamu; Sousa, Fabiano Luis de; Garcia, Ezio Castejon

Multiobjective and Multicase Optimization of a Spacecraft Radiator

Multiobjective and Multicase Optimization of a Spacecraft Radiator

Douglas Felipe da Silva[1]*, Issamu Muraoka[1], Fabiano Luis de Sousa[1], Ezio Castejon Garcia[2]

Silva DF (iD) https://orcid.org/0000-0002-3061-0016
Muraoka I (iD) https://orcid.org/0000-0001-7442-7179
Garcia EC (iD) https://orcid.org/0000-0001-9058-8853

ABSTRACT: Optimization is now an established tool for obtaining better solutions in engineering design. Nevertheless, the multiplicity of possible applications and the continuing search for better computational performance has motivated researchers in continuing to propose new methods, as well as improvements on existing ones. Not only optimization has allowed a better exploration of the design space, it also can significantly reduce the time of the design process. In this paper the advantages of using a fully multiobjective and multicase approach for the design of space radiators is presented. The optimization of Amazonia-1 satellite batteries panel thermal design is investigated. Instead of conventional space radiators, in this work an innovative solution considering the fin as heat absorber is analyzed. The results have shown that there are several viable configurations regarding to fin coating material, heater power consumption and additional mass, and the choice of the appropriate radiator configuration shall be evaluated based on system impact. The possibility of testing automatically different coatings and sizes for the fin, allowed by the optimization approach, increased significantly the probability of finding viable solutions on the design space.

KEYWORDS: Optimization, Thermal design, Satellite thermal control.

INTRODUCTION

Satellite thermal control is intended to produce suitable temperature conditions for all satellite subsystems. These have reliable performances only within specific temperature ranges and, if the temperature is not restricted within these ranges, poor performance or permanent damage to the subsystem may occur.

To ensure successful thermal control, the spacecraft should be designed such that the heat generated by each component is ultimately radiated into deep space with a temperature of approximately 2.7 K. Because the thermal radiator is the primary heat flow path between the spacecraft and deep space, most spacecraft are equipped with one or more radiators. Generally, the radiators are passive devices and known for their high reliability. This is the most important requirement in spacecraft design because it is impossible to retrieve or repair the spacecraft once it is launched. Minimizing the weight and power consumption of the radiator is also important because of their direct association with the cost (Gilmore 2002).

Optimization has already been applied in the design of space radiators. Kim *et al.* (2015) present a radiator design optimization based on two different approaches: the first method combines an optimization algorithm with thermal analysis; the second method is a stepwise approach that adds a radiator node with the highest temperature sensitivity until the temperature limits are satisfied. A thermal model of a small spacecraft was developed to verify the proposed optimization methods, and test problems of various

versions of the thermal model were appropriately defined. The numerical optimal solutions for the test problems using these methods showed good agreement with the analytic solutions.

Kim *et al.* (2017) investigated the optimization of a spacecraft radiator, formed in a honeycomb structure, designed to enhance the thermal performance while reducing its mass. The design guidelines for radiator configurations, such as the distance between heat pipes, facesheet thickness, and honeycomb core density, were suggested. To derive the analytic solution of the governing equation, a linear approximation was used and the accuracies of the solutions were verified with a fourth-order finite-difference method. The heat rejection rate that minimizes mass per unit heat rejection and the pertinent radiator shape was also presented. Although the honeycomb core density hardly influenced the distance between the heat pipes, it played an important role in determining the facesheet thickness. It was directly associated with the structural stiffness of the radiator, and thereby a crosscheck evaluation in structural aspect was necessary. All of the processes for optimization were applied to three different surface treatments (OSR, silverized Teflon, and white paint Z93 C), and it was shown that Z93 C had the highest efficiency.

Sam and Deng (2011) presented an optimized thermal design of a geostationary communications satellite panel. The optimization was performed for a worst hot case scenario employing the optimization feature of SINDA/FLUINT commercial software. Four radiator areas were sized instead of a centralized one in order to improve the heat rejection to space. The placement and size of the radiators were determined according to the component's distribution and their heat dissipation. Also, the thermal model was parameterized to optimize the heat pipe embedded network size. The length of the heat pipes were the design variables selected for the optimization and the objective function minimized was the total weight of the heat pipe network. As an optimal solution, the minimized total weight of the heat pipe network was 5.87 kg; the weight saved was 1.5 kg in comparison with the initial approach. SINDA/FLUINT optimization feature is restricted to just one case of analysis at time, for example hot case or cold case, and to continuous variables.

Afshari *et al.* (2017) analyzed the mass optimization of a radiator for a mechanically pumped fluid loop system in a geosynchronous orbit satellite. The non-dominated sorting genetic algorithm (NSGA-II) was used for minimizing the total mass and pressure drop by considering a constant transferred heat rate at the heat exchanger. The amount of transferred heat and wasted energy due to the pressure drop inside the pipe was considered as a function of the geometrical parameters (pipe length and internal diameter). The results have shown that by increasing the pipe diameter the pressure drop decreases while the total mass increases and, consequently, the optimum condition is a compromise between the minimum mass and pressure drop for the constant value of the transferred heat.

As the satellite thermal analysis involves at minimum two cases, hot and cold, and the solution is a trade-off between the design parameters, a better approach is to consider it as a multiobjective problem, as done by Muraoka *et al.* (2006). In that work, minimization of heater power consumption and satellite equipment temperature excursions were posed as objectives. Though considering two objectives, they formulated and solved the problem as mono-objective, by combining the two objective functions into a single one using weights. This approach has the advantage of allowing the use of the many existing nonlinear search algorithms to solve the problem, but for a given set of weights it returns only one point of the Pareto frontier (a set of non-dominated solutions, being chosen as optimal, if no objective can be improved without sacrificing at least one other objective), and is not capable of retrieving the entire frontier if it has non-convex regions, according to Messac *et al.* (2000). From the designer's point of view, it is interesting to know the entire Pareto frontier, so a better judgment of the possible trade-off solutions can be made. In fact, the satellite thermal designer would benefit a lot from a tool that automatically searches the design trade space for candidate optimal solutions, both from the point of view of increasing the possibility of finding a more suitable solution to the problem at hand, as well as in saving design time by automating the analysis process.

In this paper such approach is highlighted through the multiobjective and multicase design optimization of Amazonia-1 satellite batteries panel and, differently from the works of Krikkis and Razelos (2002), Kumar *et al.* (1993) and Naumann (2004) in which the fin optimization was intended to increase the heat rejection process, an innovative approach based on fin employment to perform as a solar collector is presented. Here an enhanced version of the M-GEO optimization algorithm used by Muraoka *et al.* (2006) is coupled to a commercial thermal analysis software through a customized spreadsheet interface, from which the design parameters are set, execution controlled and results retrieved. It also embodies the optimization algorithm.

OPTIMIZATION TOOL

The optimization tool uses the structure of C&R Technologies® Thermal Desktop® and SINDA/FLUINT software package coupled to Excel®, with the following functions:

- Excel® works as an interface that manages the execution, supplies control parameters and receives the results;
- Thermal Desktop® pre-process the data for the solver by calculating the radiative and conductive coupling factors and the external radiation heat for a given orbit and attitude; and
- SINDA/FLUINT calculates the temperatures by solving the heat balance equation system.

C&R Tech's software thermal modeling is based on nodal or lumped parameter method. In this method the satellite is divided in a number of regions, assumed isothermal, which are called nodes. These nodes exchange heat between each other by conduction and radiation and with space by radiation. Also, they can receive heat loads from external sources or from electronic components. The temperature of each node is the result of these interactions. The governing equation is the energy equation, which consists of transient, conduction, and radiation terms plus boundary conditions (solar radiation, albedo and Earth radiation) as source term. This equation can be written as presented in Eq. 1 by Karam (1998):

$$(mcp)_i \frac{dT_i}{dt} = Q_i^D + (\alpha Q^S + \alpha Q^A + \varepsilon Q^E)_i - \sum_{j=1}^{n} K_{ij}(T_i - T_j) - \sum_{j=1}^{n} \sigma R_{ij}(T_i^4 - T_j^4) \tag{1}$$

where the thermal mass is mcp (J/K); the external incident loads are Q^S, Q^A, and Q^E (W), while internal heat dissipation is Q^D [W]; the conduction and radiation exchange factors are represented by K_{ij} (W/K) and R_{ij} (m^{-2}), respectively; the Stefan-Boltzmann constant is σ (W/m²/K⁴); and T_i and T_j (K) are the temperatures of nodes i and j, respectively.

A recent enhanced version of M-GEO multiobjective evolutionary algorithm developed by Galski et al. (2005) was used as the search engine. It can deal with design spaces containing continuous and discrete variables, and has already been used successfully for the optimal design of spacecraft equipment layout, as presented by Lau et al. (2014). The optimization algorithm was embedded into the already existing Excel® to Thermal Desktop® interface spreadsheet as a VBA® (Visual Basic for Applications) script. This modified spreadsheet executes the thermal analysis software control by imputing the design variables (based on optimization algorithm), instructing the execution of the analysis cases, receiving output data and evaluating the objective function. The thermal mathematical model in Thermal Desktop® must be parameterized by symbols, in order to make feasible the optimization process.

In Fig. 1 is shown the control interface on Excel® screen whereby the commands are executed, the input data and control parameters are inserted, the optimization process is followed and the results are presented.
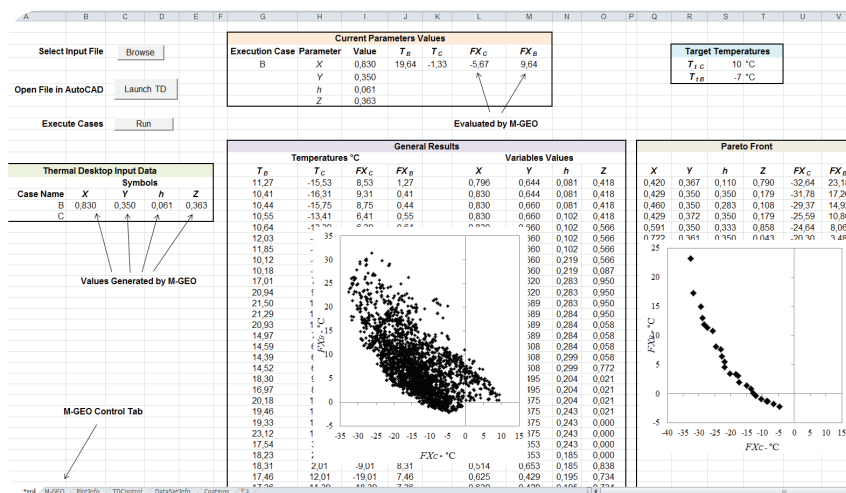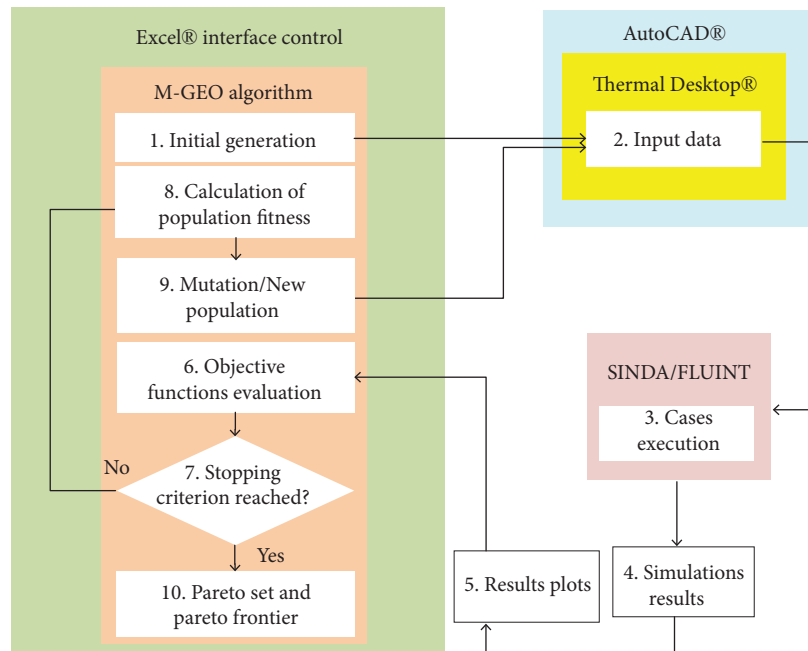

Figure 1. Optimization tool interface.

Figure 2 shows the overall structure of the optimization process in a block diagram.

Figure 2. Optimization tool structure.

APPLICATION DESCRIPTION AND DEFINITION OF THE OPTIMIZATION PROBLEM

To highlight the possibilities and features of the optimization approach described in the previous section, it was applied to the thermal design of the batteries panel of Amazonia-1 satellite. Amazonia-1 is the first satellite to use the Brazilian Multi Mission space Platform (MMP), being developed by the National Institute for Space Research (INPE), under coordination of the Brazilian Space Agency (AEB).

Amazonia-1 satellite is depicted in Fig. 3, and a few salient features are as follows:

- Overall dimensions of the main body = 2200 × 950 × 950 mm;
- Mass = ~ 500.0 kg;
- Orbit = sun-synchronous, 752.4 km high, 98.405° inclination and passage time 10:30 a.m.;
- Structure = aluminum honeycomb structure;
- Power = 420 W (average), InGAP/InGaAs/Ge solar panels, lithium ion battery;
- Stabilization = 3 axis stabilized;
- Mission life = 4 years.

The batteries panel contains the components listed in Table 1. The layout of panel's face exposed to the satellite interior is presented in Fig. 4., and exposed to space environment is shown in Fig. 5. The panel, including aluminum face sheets and a honeycomb aluminum core, has thickness of 26.5 mm, and planar dimensions of 899.2 mm × 882.0 mm.

The panel is thermally insulated from the remaining parts of the satellite conductively through fiber glass-epoxy washers, and radiatively through Multi Layer Insulation blankets (MLI). The battery packs are thermally coupled to the panel (contact area of 0.002 m² for each battery pack). Both panel's internal (the face which contains the batteries packs and is exposed to the satellite interior) and external (the face exposed to the space environment) faces are coated with MLI and some area on the external face is employed as a white painted radiator. The thermal optical properties, the coatings and MLI used in the panel, are summarized in Table 2.
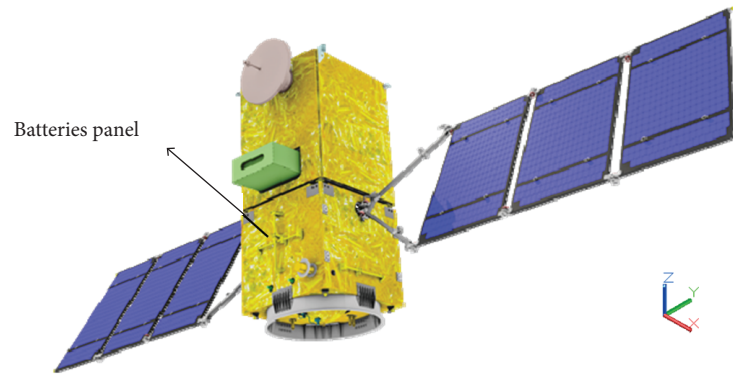
Figure 3. Amazonia-1 satellite.
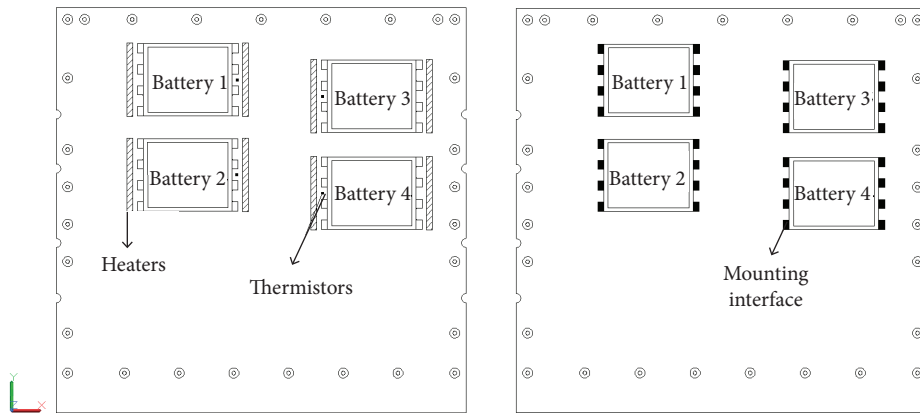
Figure 4. Batteries panel internal layout.

Table 1. Equipment temperature limits and heat dissipation.

Equipment	Temperature range (°C)	Temperature (°C)	
		Max	Min
Battery (×4)	−10 ~ 20*	2.3	2.3
Magnetotorquer (×2)	− 10 ~ 50	2.7	0
Magnetotorquer (×2)	− 80 ~ 55	0	0

*At mounting interface.

Table 2. Coatings and MLI thermal optical properties.

Coating	Emissivity (ε)		Absorptivity (α)		Effective emissivity
	BOL	EOL	BOL	EOL	
Black Paint MAP® PU1	0.88	0.88	0.95	0.95	-
*MLI	0.80	0.80	0.41	0.51	0.02
White Paint MAP® SG121FD	0.94	0.85	0.20	0.33	-

*Outer layer emissivity and absorptivity.

In order to avoid that the temperature at the batteries panel goes below −10 °C, heaters are placed near the batteries mounting interfaces. The temperatures at the panel are monitored by four thermistors, placed near the heaters. The heater circuits are

controlled by ON/OFF commands from the onboard computer. The main circuits turn on at –8 °C and turn off at –6 °C, while the redundant ones turn on at –10 °C and turn off at –8 °C. This temperature refers to the lowest value among the four thermistors.

The thermal design philosophy is to find the critical cases and analyze them supposing that all other cases result in intermediate temperatures. Three critical cases are evaluated: nominal cold (A), nominal hot (B), and emergency (C).

In cases A and B, the satellite -Y face (batteries panel) will be pointing towards Earth. In case C the satellite -Z face is permanently oriented towards the Sun with the solar rays parallel to the batteries panel. This case represents the situation in which the batteries panel will be subjected to the lowest temperature level, due to the lack of the permanent IR radiation from Earth and no incidence of direct solar radiation on it. Details of Amazonia-1 satellite thermal design are presented in the work of Silva *et al.* (2014).

For typical external heat load conditions for cold and hot conditions, and considering minimum and maximum equipment heat dissipation respectively in these two states, steady state equilibrium temperatures can be estimated for a given radiator area and guard heater dissipation. In the usual thermal design procedure (with no use of numerical optimization), the radiator area is calculated for the hot case and, then, is verified if the temperatures at cold case are above the minimum required. If not, heater power is applied accordingly, to raise the temperature to an accepted level. Using this procedure, a white painted radiator with a total area of 0.432 m² (0.8 m × 0.54 m) was estimated for the batteries panel, considering cold and hot boundary conditions, which resulted in equilibrium temperatures and guard heater power consumptions, as shown in Table 3.

Table 3. Parameters and results of evaluated cases.

| Parameter	Case A	Case B	Case C
Albedo (%)	34	42	34
Earth radiation (W/m²)	208	233	208
Solar radiation (W/m²)	1326	1418	1326
Equipment dissipation (W)	min	max	min
Predicted Temperature (°C)	–7.0*	15.6	–7.0 *
Heater Power Consumption (W)	1.4	0	32.4

*Mounting interface temperature controlled by electrical heaters.

From Table 3 it can be seen that Cases A and C require heater power to maintain the batteries panel temperature above the minimum required (–7 °C). The heater consumption in Case C is indeed very high for a satellite with the size of Amazonia-1, making desirable a thermal redesign of the batteries panel.

The satellite attitude during Case C precludes the incidence of solar radiation over the batteries panel (since the solar rays are parallel to its surface), and a possible solution for reducing the heat power consumption would be the installation of a thermal louver over the batteries panel radiator, so that heat rejection to space would be significantly reduced. Another possibility would be installing a black painted fin perpendicular to the panel, so that heat could be collected from the solar rays to warm the panel. Both solutions would add mass to the satellite, which should be avoided, but the second one would be much simpler and reliable from the mechanical point of view, since it has no moveable parts in contrast with thermal louvers.

For the present study the fin solution is adopted and the problem is to find a configuration that reduces, ideally to zero, the need for heater consumption, minimizing the additional mass to the satellite. Moreover, the installation of the fin should have minimal impact, if any, in the radiator temperature in Case B. Figure 5 shows a possible fin positioning over the panel.

The thermal design problem can then be posed as: by varying the radiator's area (X and Y) and fin's height (h), minimize the difference between the design temperatures calculated for cases B and C and the respective maximum and minimum temperatures allowed for the radiator. These are the temperature constraints for the problem, T_{max} and T_{min}. They were set to 10 °C and –7 °C for cases B and C, respectively.
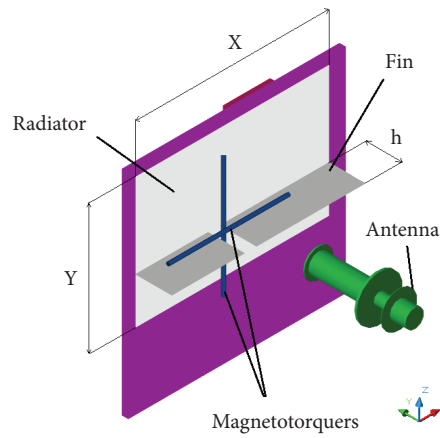
Figure 5. Fin disposition over the batteries panel, and geometric design parameters.

Mathematically, the optimization problem can be formulated as follows:

Minimize (Eqs. 2 and 3):

$$FX_B(X,Y,h) = T_B - T_{max} \tag{2}$$

$$FX_C(X,Y,h) = T_{min} - T_C \tag{3}$$

Subjected to (Eqs. 4 to 8):

$$X_{min} \leq X \leq X_{max} \tag{4}$$

$$Y_{min} \leq Y \leq Y_{max} \tag{5}$$

$$h_{min} \leq h \leq h_{max} \tag{6}$$

$$T_B \leq T_{max} \tag{7}$$

$$T_{min} \geq T_C \tag{8}$$

where FX_B = objective function for case B (°C); T_{max} = constraint temperature for case B (10 °C); T_B = hottest sensor temperature for case B (°C); FX_C = objective function for case C (°C); T_{min} = constraint temperature for case C (–7 °C); T_C = coldest sensor temperature for case C (°C); X = radiator length (between 0.37 m and 0.83 m); Y = radiator width (between 0.35 m and 0.66 m); h = fin height (between 0.05 m and 0.35 m).
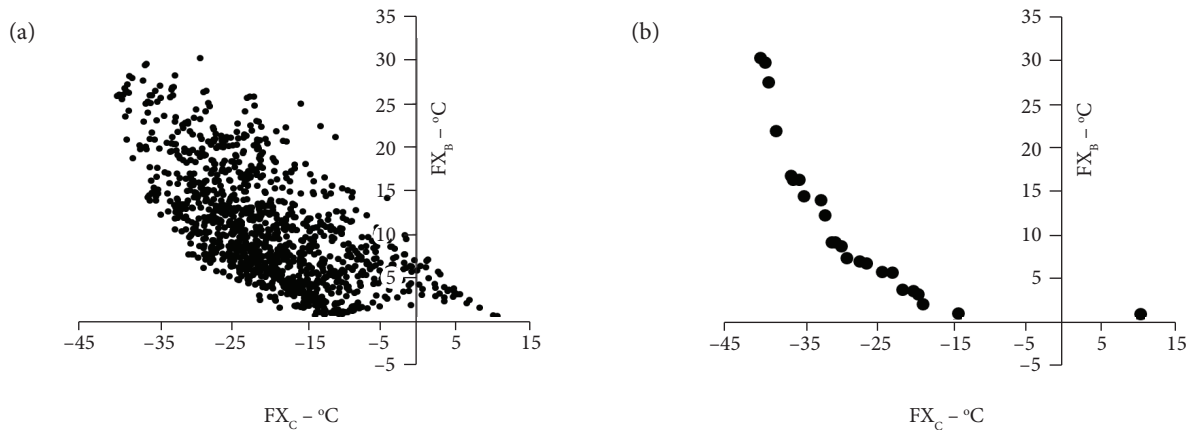
RESULTS

The optimization tool was set to search for solutions that minimize simultaneously the objective functions defined in Eqs. 2 and 3, from a set of random initial values for the design variables.

As the fin main purpose is to perform as a solar collector, the first considered coat for it was MAP® PU1 black paint. In order to avoid high temperatures in hot case (case B), only the fin face pointed to the Sun is black coated, while the remaining faces are

white painted. For the fin thickness was set a constant value of 2 mm. Figures 6a and 6b, show, respectively, the objective functions for Cases B and C found for 1200 design points simulated and the Pareto frontier obtained.

Figure 6. (a) All results found during the search, with the fin face pointed to the Sun black painted, and (b) Pareto frontier.

As shown in Fig. 6a, no viable solution was found that satisfies both temperature restrictions, what would imply in zero or negative values for FX_B and FX_C. In fact, only solutions that satisfy the temperature restriction for the emergency case (Case C) were found. All values of FX_B are positive, meaning that all temperatures are above the maximum constraint value of 10 °C in hot case (Case B). Based on these results and trying to reduce the temperature in the hot case, the solution with fin white painted in both faces was analyzed. The results are shown in Figs. 7a and 7b.
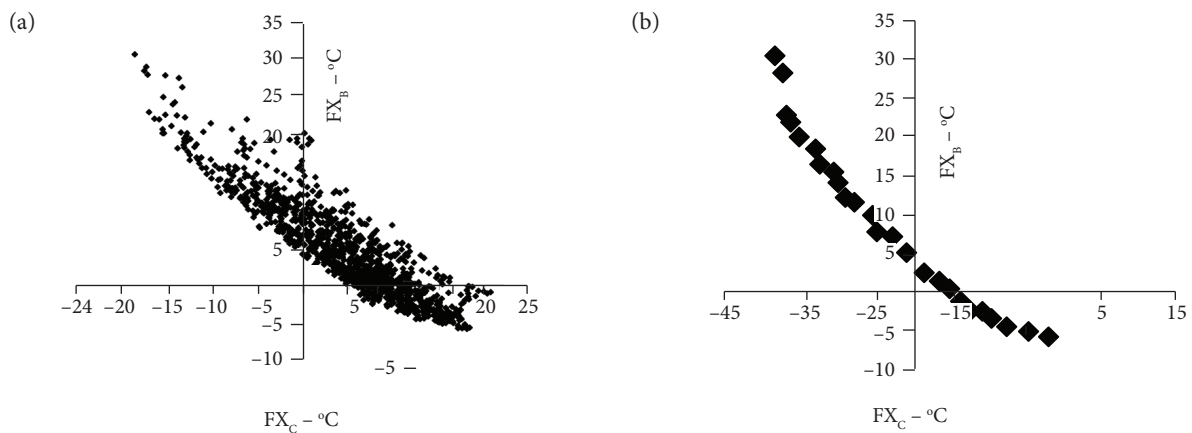

Figure 7. (a) All results found during the search, with the fin white painted, and (b) Pareto frontier.

By analyzing Figs. 7a and 7b it can be noted that both temperature restrictions can be satisfied, but not simultaneously. However, from the engineering point of view, for a given solution that satisfies the high temperature restriction, a viable solution can be achieved also for the emergency case, if additional heater power can be employed to raise the temperature until the required level. This means that the points at the right-bottom quadrant of Figs. 7a and 7b, can be moved to the left-bottom quadrant, just heating adequately the radiator during the emergency case.

For all solutions positioned at the right-bottom quadrant of Fig. 7a, was calculated the heater power needed to make $FX_C = 0$ for the emergency case. The results are shown in Figs. 8a and 8b, in terms of heater consumption and fin mass. As can be seen in

Figs. 8a and 8b there are many possibilities to be chosen and the appropriate radiator configuration to be implemented, regarding to additional mass or power consumption, should be evaluated based on system impact.
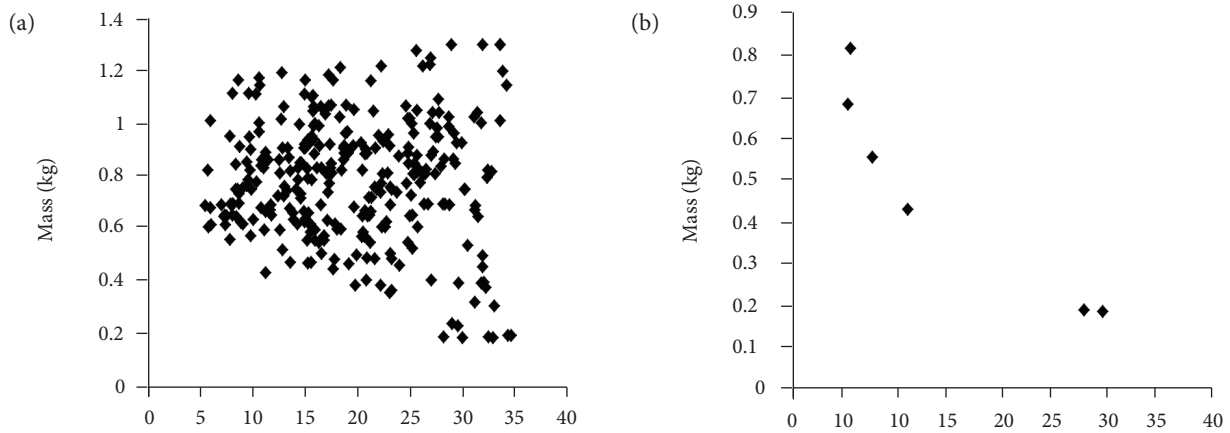
Figure 8. (a) Fin mass and heater power consumption for a set of radiator solutions with white painted fin, which satisfy temperature restrictions in hot and emergency cases simultaneously, and (b) Pareto frontier.

As the previously simulation results showed, the coating of the fin side facing the Sun may have a significant impact in finding design solutions that would satisfy simultaneously both temperature restrictions. Hence, the optimization problem was modified such that the coating is now treated as a design variable, named Z. Hence, FX_B and FX_C are now functions of the variables X, Y, h and the new discrete variable Z (Eq. 9):

$$Z = Zi, \text{ where } i = 1 \text{ to } N \tag{9}$$

For the present work, ten different coatings where considered for variable Z, as presented in Table 4. The optical properties of these coatings were obtained from Gilmore (2002).

Table 4. Coatings and thermal optical properties.

| Item (i)	Coating	α	ε	α/ε
1	Polished Aluminum	0.15	0.05	3.00
2	Polished Stainless Steel	0.42	0.11	3.82
3	NASA/GSFC NS-53-B green paint	0.52	0.87	0.60
4	NASA/GSFC NS-55-F green paint	0.57	0.91	0.63
5	Sandblasted Stainless Steel	0.58	0.38	1.53
6	Black Anodize	0.65	0.82	0.79
7	Green Anodize	0.66	0.88	0.75
8	Fiberglass Epoxy	0.72	0.89	0.81
9	NASA/GSFC dark mirror, SIO-Cr-Al	0.86	0.04	21.5
10	Ebanol C Black	0.97	0.73	1.33

Results for the modified optimization problem, considering the coating of the fin side facing the Sun as an additional design variable, are shown in Figs. 9a and 9b.

(a)

(b)
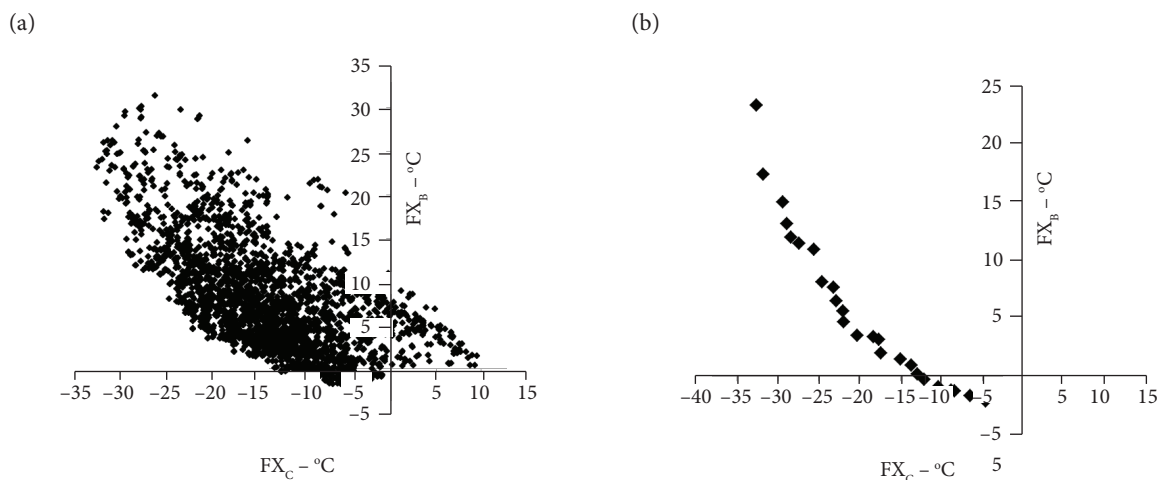
Figure 9. (a) Search results considering the coating of the fin side facing the Sun as an additional design variable, and (b) Pareto frontier.

By analyzing Fig. 9a it can be noted that several configurations, represented by the points at the left-bottom quadrant, comply with both temperature constraints. That is, using coatings shown in Table 4, viable designs for the radiator can be achieved without the need of using heaters in the emergency case. Figure 9b shows the six non-dominated viable solutions for the problem. In Figs. 10a and 10b the viable solutions are shown in terms of radiator area, mass and fin coating. While all coatings shown in Table 4 can be used to provide viable radiator designs, only coatings 2, 4 and 10 provide non-dominated solutions, making them more suitable to be considered for covering the fin.

From the mass point of view, coating 10 (Ebanol C Black) is the best coat, with approximately 0.7 kg. If compared to the results for the original radiator thermal design without fin, shown in Table 3, the results of the optimization process indicated that the heater power consumption of 32.4 W can be exchanged by an addition of approximately of 0.7 kg in satellite mass. The increase of such a small amount of mass in exchange of such amount of power consumption is clearly advantageous for satellites of Amazonia-1 class. This result shows the great improvements that can be made in satellite radiator design using the approach presented in this paper.

(a)

(b)
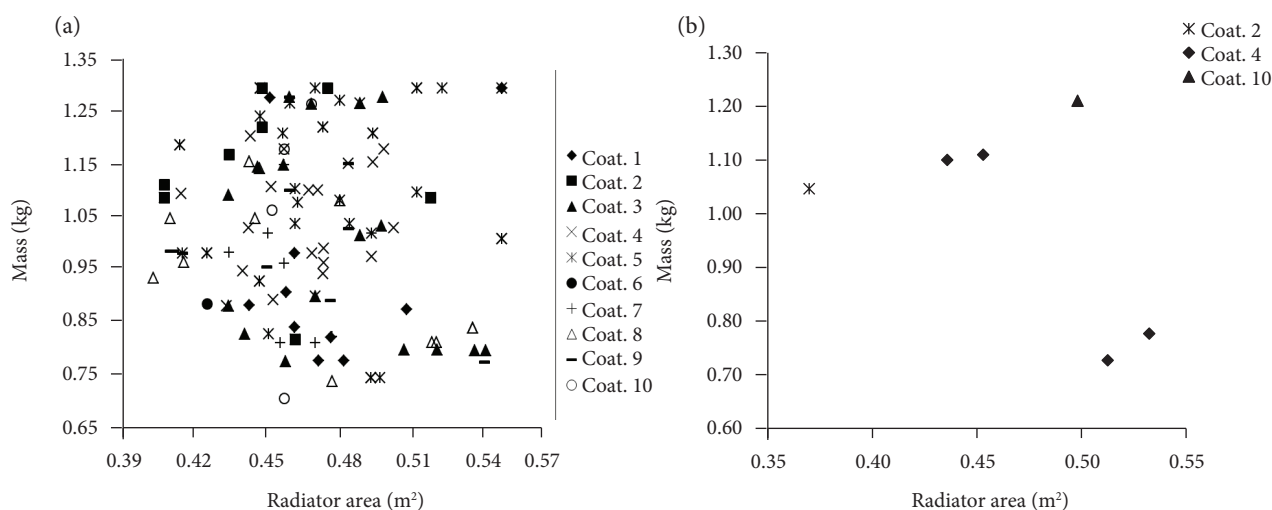
Figure 10. (a) Radiator area and mass of all viable solutions, and (b) Non-dominated solutions.

CONCLUSIONS

In this paper the advantages of using a fully multiobjective multicase approach for the design of space radiators was shown. The optimization runs were performed by customizing an already existing procedure/tool that couples Thermal Desktop® and SINDA/FLUINT thermal software to Excel®. While the spreadsheet is used as interface for input data, output of results, control of optimization parameters and host to a multiobjective algorithm, calculations of the thermal parameters are done in the thermal software.

Applied to the optimization of the thermal design of the batteries panel of Amazonia-1 satellite, the approach not only allowed the automatic creation of non-dominated (trade-off) solutions, providing different design options for implementation, but also led to a substantial reduction on design process time, since it works autonomously and covers a wide range of design possibilities, including working with discrete variables. The results have shown that the hater power consumption of 32.4 W can be exchanged by an addition of 0.7 kg in satellite mass, for the fin coated with Ebanol C Black. Also, there are several viable configurations regarding to fin coating material, heater power consumption and additional mass, and the choice of the appropriate radiator configuration shall be evaluated based on system impact.

Finally, it is noteworthy to mention how using optimization can also help on the assessment of innovative design proposals. In this paper, a fin was added to the radiator not to increase the area of heat rejection, as in a traditional radiator design, but as a way to increase the heat absorption from the Sun in the emergency case. The possibility of testing automatically different coatings and sizes for the fin, allowed by the optimization approach, increased significantly the chance of finding viable solutions on the design space, what actually happened in this paper's example. These solutions proved not only to be viable on the context of the formulated optimization problem, but also to be a significant improvement, regarding heater power savings, over the original, non optimized, radiator design.

AUTHOR'S CONTRIBUTION

Conceptualization, Silva DF, Muraoka I and De Sousa FL; Methodology, Silva DF, Muraoka I and De Sousa FL; Investigation, Silva DF, Muraoka I and Garcia, EC; Writing – Original Draft, Silva DF; Writing – Review and Editing, Silva DF, Muraoka I, De Sousa FL and Garcia, EC.

REFERENCES

Afshari BM, Abedi M, Shahryari M (2017) Optimization of a radiator for MPFL system in a GEO satellite. Advances in Aircraft and Spacecraft Science 4(6):701-709. https://doi.org/10.12989/aas.2017.4.6.701

Galski RL, De Sousa FL, Ramos FM (2005) Application of a new multiobjective evolutionary algorithm to the optimum design of a remote sensing satellite constellation. Presented at: 5th International Conference on Inverse Problems in Engineering: Theory and Practice; Cambridge, UK.

Gilmore DG, editor (2002) Spacecraft thermal control handbook. El Segundo: The Aerospace Press.

Karam RD (1998) Satellite thermal control for system engineers. Cambridge: Progress in Astronautics and Aeronautics.

Kim H-K, Choi S, Park S, Lee KH (2015) Node-based spacecraft radiator design optimization. Advances in Space Research 55(5):1445-1469. https://doi.org/10.1016/j.asr.2014.09.007

Kim TY, Chang S-Y, Yong SS (2017) Optimizing the design of space radiators for thermal performance and mass reduction. Journal of Aerospace Engineering 30(3):04016090. https://doi.org/10.1061/(ASCE)AS.1943-5525.0000676

Krikkis RN, Razelos P (2002) Optimum design of spacecraft radiators with longitudinal rectangular and triangular fins. Journal of Heat Transfer 124(5):805-811. https://doi.org/10.1115/1.1497359

Kumar SS, Nayak V, Venkateshan SP (1993) Optimum finned space radiators. International Journal of Heat and Fluid Flow 14(2):191-200. https://doi.org/10.1016/0142-727X(93)90028-L

Lau V, De Sousa FL, Galski RL, Rocco EM, Becceneri JC, Santos WA, Sandri SA (2014) A multidisciplinary design optimization tool for spacecraft equipment layout conception. Journal of Aerospace Technology and Management 6(4):431-446. https://doi.org/10.5028/jatm.v6i4.399

Messac A, Sundararaj GJ, Tappeta RV, Renaud JE (2000) Ability of objective functions to generate points on nonconvex Pareto frontiers. AIAA Journal 38(6):1084-1091. https://doi.org/10.2514/2.1071

Muraoka I, Galski RL, De Sousa FL, Ramos FM (2006) Stochastic spacecraft thermal design optimization with low computational cost. Journal of Spacecraft and Rockets 43(6):1248-1257. https://doi.org/10.2514/1.20066

Naumann RJ (2004) Optimizing the design of space radiators. International Journal of Thermophysics 25(6):1929-1941. https://doi.org/10.1007/s10765-004-7747-0

Sam KFCH, Deng Z (2011) Optimization of a space based radiator. Applied Thermal Engineering 31(14-15):2312-2320. https://doi.org/10.1016/j.applthermaleng.2011.03.029

Silva DF, Muraoka I, Garcia EC (2014) Thermal control design conception of the Amazonia-1 satellite. Journal of Aerospace Technology and Management 6(2):169-176. https://doi.org/10.5028/jatm.v6i2.320